Organometallics **1991**, *10*, 851-860

Metallocene-Bridged Cryptands. 2. Solid-State Studies of Some Ferrocene Amides and Their Cryptand Analogues

Martin C. Grossel,*,† Mark R. Goldspink,† Joseph A. Hriljac,‡ and Simon C. Weston†

Chemistry Department, Royal Holloway and Bedford New College, University of London, Egham, Surrey TW20 0EX, U.K., and Chemical Crystallography Laboratory, University of Oxford, 9 Parks Road, Oxford OX1 3BQ, U.K.

Received December 18, 1989

Solid-state studies including magic angle spinning (MAS) NMR of several 1,1′-disubstituted ferrocenes and two X-ray structural studies aimed at increasing the understanding of the ion-binding properties of crown ether ferrocenophanes, in particular 1,1′-[(1,4,10,13-tetraoxa-7,16-diazacyclooctadecane-7,16-diyl)dicarbonyl]ferrocene dihydrate (1), and several related simple systems are reported. Crystals of 1, which are monoclinic, with a = 8.833 (7) Å, b = 21.304 (2) Å, c = 13.253 (2) Å, β = 95.24 (3)°, space group $P2_1/n$, Z = 4, R = 3.43% (R_w = 2.94%), also contain 2 molecules of water per asymmetric unit. These are interlaced between the ferrocenophanes and link the structure through a hydrogen-bonded network. The crown ether is highly distorted and compressed with only the ether oxygens available for complexing, indicative of poor ion-binding ability as confirmed by solvent extraction and spectroscopic experiments. However, there is evidence from the latter for the formation of 1:1 and 2:1 (guest:host) complexes of 1 with Li$^+$ salts. Crystals of 1,1′-bis(*N*-methylcarbamyl)ferrocene (4a), a simple model for 1, are monoclinic, with a = 32.672 (2) Å, b = 5.962 (4) Å, c = 13.358 (1) Å, β = 104.088 (6)°, space group $C2/c$, Z = 8, R = 4.56% (R_w = 5.98%). This represents the first structural report of a simple ferrocene amide.

Introduction

The incorporation of a redox center into a crown ether or cryptand complex offers a route to ion-selective optical and electronic detectors.[1] One approach to such structures which has proved to be synthetically viable uses metallocenes, particularly ferrocene, as a bridging unit.[2-11] Simple ferrocene amide crown ethers show little, if any, complexing ability for group I or II metal cations,[5] but the [2.2]ferrocene cryptand, [Fc.2.2], 1, which is readily prepared[6] by reaction of 1,1′-bis(chlorocarbonyl)ferrocene with diaza-18-crown-6, has been reported to be an ion-selective binding agent.[5] A dimer, [Fc.(2,2);(2,2).Fc], 2, which can be obtained in moderate, temperature-dependent yield from this reaction,[11,12] may also have useful properties. Several polyoxa- and polyoxathiaferrocenophanes have been prepared.[7,8] These have been found to bind transition-metal cations more effectively than the corresponding simple crown ethers. Recently, a pentaoxa[13]ferrocenophane (3) has been used for redox-driven sodium ion transport across a membrane.[10]

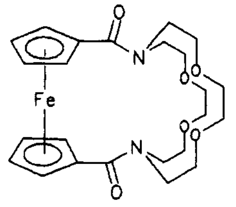

1

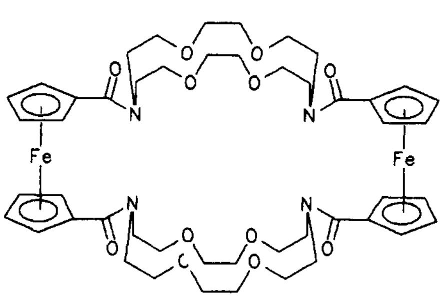

2

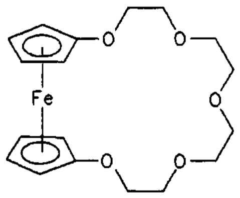

3

The cryptands 1 and 2 have been fully characterized by solution NMR spectroscopy,[6] but only recently have X-ray structural data, which allows a better assessment of their binding properties, been reported.[12,13] We now present the results of X-ray structural studies of 1 and a simple model system, 1,1′-bis(methylcarbamyl)ferrocene (4a), since no structural information on such a compound has,

---

† University of London.

‡ University of Oxford.

(1) *Chemical Sensors*; Edmonds, T. E., Ed.; Blackie: London, 1988.

(2) Oepen, G.; Vögtle, F. *Liebigs Ann. Chem.* **1979**, 1094.

(3) Biernat, J. F.; Wilczewski, T. *Tetrahedron* **1980**, *36*, 2521.

(4) Sato, M.; Watanabe, H.; Ebine, S.; Akabori, S. *Chem. Lett.* **1982**, 1753.

(5) Bell, A. P.; Hall, C. D. *J. Chem. Soc., Chem. Commun.* **1980**, 163.

(6) Hammond, P. J.; Bell, A. P.; Hall, C. D. *J. Chem. Soc., Perkin Trans. 1* **1983**, 707.

(7) (a) Akabori, S.; Habata, Y.; Sato, M. *Bull. Chem. Soc. Jpn.* **1984**, *57*, 68. (b) Akabori, S.; Shibahara, S.; Habata, Y.; Sato, M. *Bull. Chem. Soc. Jpn.* **1984**, *57*, 63. (c) Akabori, S.; Habata, Y.; Sakamoto, Y.; Sato, M.; Ebine, S. *Bull. Chem. Soc. Jpn.* **1983**, *56*, 537.

(8) (a) Bellon, P. L.; DeMartin, F.; Scatturin, V.; Czech, B. P. *J. Organomet. Chem.* **1984**, *265*, 65. (b) Bernal, I.; Raabe, E.; Reisner, G. M. *Organometallics* **1988**, *7*, 247. (c) Bernal, I.; Reisner, G. M.; Bartsch, R. A.; Holwerda, R. A.; Czech, B. P. *Organometallics* **1988**, *7*, 253.

(9) Hammond, P. J.; Beer, P. D.; Dudman, C.; Banks, I. P.; Hall, C. D.; Knychala, J. P.; Grossel, M. C. *J. Organomet. Chem.* **1986**, *306*, 67 and references therein.

(10) Saji, T.; Kinoshita, I. *J. Chem. Soc., Chem. Commun.* **1986**, 716.

(11) Hammond, P. J.; Beer, P. D.; Hall, C. D. *J. Chem. Soc., Chem. Commun.* **1983**, 1161.

(12) (a) Grossel, M. C.; Goldspink, M. R.; Knychala, J. P.; Cheetham, A. K.; Hriljac, J. A. *J. Organomet. Chem.* **1988**, *352*, C13. (b) We have completed a second structure determination of 2: Grossel, M. C.; Goldspink, M. R.; Hriljac, J. A. To be published. (c) Goldspink, M. R. Ph.D. Thesis, University of London, June 1988.

(13) Beer, P. D.; Bush, C. D.; Hamor, T. A. *J. Organomet. Chem.* **1988**, *339*, 133.

0276-7333/91/2310-0851$02.50/0

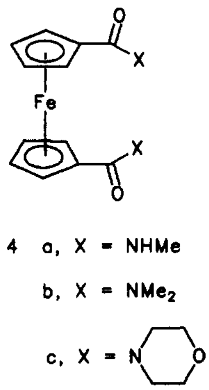

4 a, X = NHMe

b, X = NMe_2

c, X =

as yet, been described. We also report ^{13}C solid-state NMR data for a series of related ferrocene compounds together with the results of experiments concerning ion extraction and cryptate formation by 1. Finally, we describe the isolation and characterization of several 1:1 stoichiometry cryptates of 1 with several lithium salts, together with evidence for the formation of 2:1 (host:guest) complexes.

Experimental Section

Instrumentation. Solid-state ^{13}C NMR data were recorded by using a Bruker MSL 300 spectrometer fitted with a 7-mm double air bearing probe. Solution NMR spectra were recorded on Jeol FX90Q and FX270 and Bruker WH250 and WH400 spectrometers. Mössbauer spectra were recorded on a Cryophysics MS103 spectrometer with a ^{59}Co source in a rhodium matrix.

Preparation of Materials. Unless otherwise stated, spectra on known materials were in accord with those previously reported, and therefore, solution ^{13}C NMR spectral data only are quoted on known materials where required for comparison with solid-state ^{13}C NMR data.

1,1′-[(1,4,10,13-Tetraoxa-7,16-diazacyclooctadecane-7,16-diyl)dicarbonyl]ferrocene (1), i.e., [Fc.2.2], was prepared following the procedure of Hall and co-workers.[5]

1,1′-Bis(*N*-alkylcarbamyl)ferrocenes were prepared by reaction of 1,1′-bis(chlorocarbonyl)ferrocene with excess amine to give **4a–c**. (i) **1,1′-Bis(*N*-methylcarbamyl)ferrocene (4a)**:[14] IR ν_{max} (Nujol) 3312 (N–H), 1631 (C=O) cm^{-1}; ^{13}C NMR δ ($CDCl_3$) 41.7 (NCH_3), 70.7 ($C_{3,3',4,4'}$), 71.2 ($C_{2,2',5,5'}$), 79.1 ($C_{1,1'}$), 170.3 (C=O) ppm. (ii) **1,1′-Bis(*N*,*N*-dimethylcarbamyl)ferrocene (4b)**:[15] ^{13}C NMR δ ($CDCl_3$) 38.3 (NCH_3), 72.0 ($C_{3,3',4,4'}$), 72.9 ($C_{2,2',5,5'}$), 80.7 ($C_{1,1'}$), 170.6 (C=O) ppm. (iii) **1,1′-Bis(*N*,*N*-morpholinocarbonyl)ferrocene (4c)**:[16] yellow crystals (90%), mp 179.5 °C; ^1H NMR δ ($CDCl_3$) 3.66 (br, 16 H, CH_2CH_2), 4.40 (4 H, t, H_3, H_4), 4.60 (4 H, t, H_2, H_5) ppm; ^{13}C NMR δ ($CDCl_3$) 45.8 (NCH_2), 67.1 (OCH_2), 71.3 ($C_{3,3',4,4'}$), 72.2 ($C_{2,2',5,5'}$), 80.9 ($C_{1,1'}$), 169.1 (C=O) ppm; IR ν_{max} 1610 (C=O) cm^{-1}. Anal. Calcd for $C_{20}H_{24}N_2O_4Fe$: C, 58.29; H, 5.83; N, 6.80. Found: C, 58.32; H, 5.88; N, 6.38.

1,1′-Diacetylferrocene (5) was prepared by literature methods:[17] ^{13}C NMR δ ($CDCl_3$) 28.7 (CH_3), 71.5 ($C_{3,3',4,4'}$), 74.2 ($C_{2,2',5,5'}$), 81.1 ($C_{1,1'}$), 201.6 (C=O) ppm.

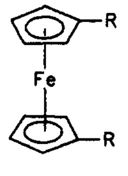

5 R = $COCH_3$

6a R = COOH

6b R = $COOCH_3$

Ferrocene-1,1′-dicarboxylic acid (6a)[18] was prepared[6] by lithiation of ferrocene[19] followed by carboxylation by use of CO_2: ^{13}C NMR δ (d_6-DMSO) 70.5 ($C_{3,3',4,4'}$), 71.8 ($C_{2,2',5,5'}$), 72.5 ($C_{1,1'}$), 170.1 (C=O) ppm. The dilithio carboxylate salt was prepared by reaction of the bisacid with LiOH, dried, and converted by reaction with oxalyl chloride[6] into 1,1′-bis(chlorocarbonyl)ferrocene: ^{13}C NMR δ ($CDCl_3$) 74.3 ($C_{3,3',4,4'}$), 75.8 ($C_{2,2',5,5'}$), 76.2 ($C_{1,1'}$), 168.5 (C=O) ppm.

Dimethyl ferrocene-1,1′-dicarboxylate (6b)[19b] was prepared by reaction of the bisacid chloride with dry methanol: ^{13}C NMR δ ($CDCl_3$) 52.4 (OCH_3), 72.3 ($C_{3,3',4,4'}$), 73.3 ($C_{2,2',5,5'}$), 80.9 ($C_{1,1'}$), 172.6 (C=O) ppm.

Ion-Complexation Studies. Attempts were made to prepare a number of cryptates of 1. These included complexes with lithium perchlorate (**12a**), lithium iodide (**12b**), and lithium trifluoromethanesulfonate (**12c**).

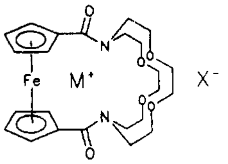

12 M^+ = Li^+

a, X^- = ClO_4^-

b, X^- = I^-

c, X^- = $CF_3SO_3^-$

In each case, cryptand 1 (1 mmol) was refluxed with the appropriate metal salt (1 mmol) in dry methanol (20 mL) for 15 min. The hot solution was filtered and allowed to cool. The complex that crystallized was separated and characterized. Reaction with lithium perchlorate gave a bright orange solid (45%): mp 127–129 °C dec; IR ν_{max} 1610 (C=O), 1112 (Cl—O) cm^{-1}; ^1H NMR δ ($CDCl_3$) 2.96, 3.29, 3.54, 3.74, 3.85, 4.08, 4.10, 4.17, 4.30, 4.47, 4.48, 4.57, 4.80 ppm; ^{13}C NMR δ ($CDCl_3$) 49.89, 51.43, 69.65, 69.85, 70.29, 71.19, 71.32, 72.40, 72.69, 73.16, 79.05, 170.88 ppm. Anal. Calcd for $C_{24}H_{32}FeN_2O_{10}LiCl$ (**12a**): C, 47.51; H, 5.36; N, 4.62. Found: C, 47.37; H, 5.20, N, 4.51. Reaction with lithium iodide gave a light tan solid (49%): mp 110–112 °C dec. Anal. Calcd for $C_{24}H_{32}FeN_2O_6LiI$ (**12b**): C, 45.45, H, 5.08, N, 4.42. Found: C, 45.27, H, 5.00, N, 4.31. Reaction with lithium trifluoromethanesulfonate gave a brown solid: mp 114–115 °C dec. Anal. Calcd for $C_{25}H_{32}FeN_2O_9LiF_3S$ (**12c**): C, 45.74, H, 4.91, N, 4.27. Found: C, 45.49, H, 4.81, N, 4.11.

Extraction Experiments. Hydroxypyridone trimethine oxonol dye salts of the alkali metals were prepared by literature methods[20] and recrystallized to a constant extinction coefficient.

In a typical procedure, 1-ethyl-3-cyano-6-hydroxy-4-methylpyrid-2-one (10 g, 0.056 mol), 1,1′,3,3′-tetramethoxypropane (4.6 g, 0.028 mol), and lithium carbonate (1.04 g, 0.014 mol) was refluxed in dry ethanol (50 mL) for 20 h. On cooling, an olive-green precipitate was formed (9.7 g, 87%), which was recrystallized from ethanol to give green cubes: mp >300 °C (lit.[20] >300 °C); IR ν_{max} (KBr) 2975–2930 (C—H), 2200 (CN), 1660 (C=O), 1615 (C=C) cm^{-1}; ^1H NMR δ (d_6-DMSO) 1.09 (6 H, t, CH_3CH_2N), 2.4 (6 H, s, CH_3Ar), 3.9 (4 H, q, CH_2N), 7.71 (2 H, d, CHAr), 9.0 (1 H, t, CH=CHCH) ppm; ^{13}C NMR δ (d_6-DMSO) 13.1 (CH_3CH_2), 18.6 (CH_3Ar), 33.8 (CH_2N), 92.2 ($C_{Ar}Me$), 110.4 ($C_{Ar}(CH)_3C_{Ar}$), 117.7 (C_N), 120.9 (CH=CHCH), 157.4 (CH=CHCH), 158.1 (CCN), 161.4 and 162.0 (C=O) ppm; UV λ_{max} 598 nm (ϵ_{max} 1.22×10^5 mol^{-1} dm^3 cm^{-1}). Anal. Calcd for $C_{21}H_{19}N_4O_4Li$: C, 63.32; H, 4.77; N, 14.07. Found: C, 63.05; H, 4.62; N, 13.89. Other dye salts were prepared in a similar manner. They had identical solution spectra,

---

(14) Sunthankar, S. V.; Mahadik, S. T. *Indian J. Chem.* **1973**, *11*, 1207.

(15) Reich-Rohnsig, P.; Schlogl, K. *Montash. Chem.* **1968**, *99*, 2175.

(16) Yang, X.; Xie, Z.; Ni, F.; Shi, S. *Fundam. Res. Organomet. Chem. Proc. China-Jpn. U.S. Trilateral Semin. Organomet. Chem., 1st 1980* **1982**, 965; *Chem. Abstr.* **1982**, *97*, 103654.

(17) (a) Rosenblum, M.; Woodward, R. B. *J. Am. Chem. Soc.* **1958**, *80*, 5443. (b) Sandstroem, J.; Seita, J. *J. Organomet. Chem.* **1976**, *108*, 371.

(18) (a) Rausch, M. D.; Fischer, E. O.; Grubert, H. *J. Am. Chem. Soc.* **1960**, *82*, 76. (b) Mayo, D. W.; Shaw, P. D.; Rausch, M. *Chem. Ind.* **1957**, 1388.

(19) (a) Rausch, M. D.; Ciappenelli, D. J. *J. Organomet. Chem.* **1967**, *10*, 127. (b) Gonsalves, K.; Zhan-ru, L.; Rausch, M. D. *J. Am. Chem. Soc.* **1984**, *106*, 3862.

(20) Grossel, M. C.; Edwards, D. J.; Cheetham, A. K.; Eddy, M. R.; Postle, S. R. *J. Mater. Chem.*, in press. See also: Farmery, D. L.; Fry, D. J.; Stonham, J. P. British Patent 1521083, 1978. Grossel, M. C.; Evans, F. A.; Weston, S. C.; Hill, R. M.; Dissado, L. A. *Chemtronics*, in press. Bland, S. W. Patent 1278621, 1972.

Table I. Summary of Crystal Data, Intensity Collection, and Data Processing

	1	4a
compd	$C_{24}H_{36}FeN_2O_8$	$C_{14}H_{16}FeN_2O_2$
M_w, g mol^{-1}	536.40	324.16
cryst shape	irregular	needle
cryst size, mm	0.11 × 0.33 × 0.33	0.09 × 0.18 × 0.44
color	orange	orange
space group	$P2_1/n$	$C2/c$
crystal system	monoclinic	monoclinic
a, Å	8.833 (7)	32.672 (2)
b, Å	21.304 (2)	5.9621 (4)
c, Å	13.253 (2)	13.358 (1)
β, deg	95.24 (3)	104.088 (6)
U, Å^3	2483.5	2523.8
Z	4	8
D_c, g cm^{-1}	1.432	1.7063
$F(000)$	1264	1344
μ, cm^{-1}	6.537	96.69
abs factors	1.0–1.05	1.00–1.86
radiation	Mo Kα	Cu Kα
λ, Å	0.710 69	1.5418
scan mode	ω–2θ	ω–2θ
T, K	294	294
2θ limits, deg	1–22.5	1–70.0
data range, hkl	$-1\rightarrow9,-1\rightarrow22,-14\rightarrow14$	$-39\rightarrow39,0\rightarrow7,-2\rightarrow-16$
scan speed range, deg min^{-1}	1.4–2.7	1.3–4.1
ω scan width, deg	$0.9 + 0.35 \tan\theta$	$1.0 + 0.14 \tan\theta$
total data	4096	6540
total unique data	3036	2393
no. of data used, $I > 3\sigma(I)$	1697	1612
R, merge, %	2.88	4.28
no. of refined params	357	182
weights[21]	4.05, 4.66, 2.63	1043, 1425, 426
final shift/esd	0.09	0.01
R, %	3.43	4.56
R_w, (%)	2.94	5.98

and the physical properties were identical with those previously reported.[20]

The dyes were recrystallized to a constant extinction coefficient prior to use in extraction experiments. In a control experiment, no evidence was found for extraction of oxonol dye from an aqueous solution into dichloromethane. Equal volumes of equimolar (ca. 1.5 × 10^{-5} mol dm^{-3}) solutions of oxonol dye (in water) and a dichloromethane solution of ionophore (1 or dibenzo-18-crown-6) were shaken 100 times at room temperature, and the mixture was then allowed to stand for 30 min (care being taken to avoid solvent evaporation). The layers were separated, and the residual concentration of the dye in the aqueous layer was determined spectrophotometrically (at λ_{max} 598 nm). Each determination was repeated 10 times.

X-ray Structural Studies

1,1′-Bis(*N*-methylcarbamyl)ferrocene (4a). An orange crystal, grown by slow evaporation of a $CHCl_3$/hexane solution and approximately 0.09 × 0.18 × 0.44 mm in size, was used for the data collection. The crystal was mounted on an Enraf-Nonius CAD4F diffractometer, and the unit cell and orientation matrix were determined by using automated search and centering routines. The final unit-cell dimensions were obtained by the least-squares refinement of the setting angles of 25 high-angle ($2\theta > 30°$) reflections. Data were collected with graphite-monochromated Cu Kα radiation with use of the scan parameters listed in Table I. Backgrounds were measured at each side of the scan for a total time equal to one-half of the peak scan. The intensities of three reflections were remeasured every 2 h as intensity standards; these indicated no substantial decay.

Table II. Fractional Atomic Coordinates with Estimated Standard Deviations for $Fe(CpCONHMe)_2$ (4a)

atom	x/a	y/b	z/c
Fe(1)	0.12601 (2)	0.2513 (1)	−0.15004 (4)
C(1)	0.1921 (1)	0.1969 (9)	0.0589 (3)
C(2)	0.0591 (1)	0.0385 (9)	−0.3325 (3)
C(3)	0.2382 (2)	−0.1053 (9)	0.1161 (4)
C(4)	0.0135 (2)	−0.2755 (10)	−0.3713 (5)
C(11)	0.1487 (1)	0.2651 (8)	0.0050 (3)
C(12)	0.1121 (1)	0.1282 (9)	−0.0207 (3)
C(13)	0.0781 (1)	0.2630 (10)	−0.0749 (4)
C(14)	0.0939 (1)	0.4816 (9)	−0.0835 (4)
C(15)	0.1376 (1)	0.4849 (8)	−0.0335 (3)
C(21)	0.1027 (1)	0.1108 (8)	−0.2910 (3)
C(22)	0.1172 (2)	0.3336 (9)	−0.3027 (3)
C(23)	0.1610 (2)	0.3396 (10)	−0.2530 (4)
C(24)	0.1732 (1)	0.1265 (10)	−0.2107 (4)
C(25)	0.1375 (1)	−0.0171 (9)	−0.2337 (3)
N(1)	0.1969 (1)	−0.0243 (6)	0.0633 (3)
N(2)	0.0542 (1)	−0.1836 (6)	−0.3213 (3)
O(1)	0.2198 (1)	0.3275 (7)	0.0945 (3)
O(2)	0.0307 (1)	0.1579 (7)	−0.3750 (3)

The data were corrected for Lorentz and polarization effects, and an empirical absorption correction based on the ψ scan data of three reflections was applied. The position of the iron atom was determined by Patterson techniques, and the remaining non-hydrogen atoms were located by difference-Fourier techniques. Hydrogen atoms were input in idealized positions (C–H = 1.0 Å) with isotropic temperature factors and were constrained to "ride" on the attached atoms during subsequent refinements. A three-term Chebyshev polynomial weighting scheme was used.[21] The last cycle of least-squares refinement converged with R = 4.56% (R_w = 5.98%). The final difference-Fourier map contained no peaks greater than 0.45 e/Å^3. Details of the data collection and refinement are summarized in Table I. Atomic coordinates are presented in Table II.

The computer programs RC85[22] and CRYSTALS[23] were used throughout.[24] Figures were drawn with CHEM-X[25] or SNOOPI.[26]

1,1′-[(1,4,10,13-Tetraoxa-7,16-diazacyclooctadecane-7,16-diyl)dicarbonyl]ferrocene Dihydrate, [Fc.2.2], 1. An orange crystal of approximate dimensions 0.11 × 0.33 × 0.33 mm was grown and mounted in the manner described above. Data were collected with graphite-monochromated Mo Kα radiation as already described and were corrected for Lorentz and polarization effects, and an empirical absorption correction based on the ψ scan data of four reflections was applied. The structure was solved by Patterson and difference-Fourier techniques. The initial identification of the oxygen atoms of the two water molecules present was based on the heights and positions of peaks in a difference-Fourier map generated after all of the remaining non-hydrogen atoms had been refined. Hydrogen atoms attached to the carbon atoms were then input in idealized positions (C–H = 1.0 Å) with isotropic temperature factors. These hydrogen atoms were constrained to remain in idealized positions during the refinement, but the isotropic temperature factors were successfully refined. Three of the four hydrogen atoms of the water molecules were located from difference-Fourier maps, and the positions were successfully refined with slack restraints on the O–H distances (1.0 ± 0.1 Å). A three-term Chebyshev polynomial weighting scheme was applied.[21] The last cycle of least-squares refinement converged with R = 3.43% (R_w = 2.94%). The final difference-Fourier map contained no features greater than 0.2 e/Å^3. These results are also summarized in Table I, with atomic coordinates listed in Table III.

Results and Discussion

X-ray Studies. 1,1′-Bis(methylcarbamyl)ferrocene (4a). A view of the molecular structure of **4a** is shown in Figure 1, and the bond lengths and angles are listed in

---

[21] Prince, E. *Mathematical Techniques in Crystallography*; Springer-Verlag: New York, 1982.

[22] Baird, P. D. Chemical Crystallography Laboratory, University of Oxford, Oxford, U.K., 1985.

[23] Watkin, D. J.; Carruthers, J. R.; Betteridge, P. W. *CRYSTALS User Guide*; Chemical Crystallography Laboratory, University of Oxford: Oxford, U.K., 1985.

[24] Atomic scattering factors were taken from: *International Tables for Crystallography*; Kynoch Press: Birmingham, 1974; Vol IV.

[25] Developed and distributed by Chemical Design Ltd., Oxford, U.K.

[26] Davies, E. K.; Baird, P. D.; Foxman, B. Chemical Crystallography Laboratory, University of Oxford, Oxford, U.K., 1987.

Table III. Fractional Atomic Coordinates with Estimated Standard Deviations for [Fc.2.2] (1)

atom	*x/a*	*y/b*	*z/c*
Fe(1)	0.04604 (9)	0.06954 (4)	0.30963 (6)
C(1)	−0.1245 (6)	0.0251 (3)	0.1028 (4)
C(2)	0.0892 (6)	0.2153 (3)	0.2768 (3)
C(11)	−0.2978 (5)	0.0683 (3)	−0.0290 (4)
C(12)	−0.4351 (6)	0.0922 (3)	0.0185 (5)
C(14)	−0.5214 (6)	0.1854 (3)	0.0948 (4)
C(15)	−0.4618 (6)	0.2488 (3)	0.1238 (4)
C(17)	−0.2627 (5)	0.2993 (3)	0.2240 (4)
C(18)	−0.1296 (5)	0.2877 (3)	0.3014 (4)
C(21)	−0.0797 (6)	0.1341 (3)	0.0433 (4)
C(22)	0.0212 (6)	0.1430 (3)	−0.0430 (4)
C(24)	−0.0293 (6)	0.2491 (3)	−0.0877 (4)
C(25)	0.0200 (6)	0.3150 (3)	−0.0627 (4)
C(27)	0.1327 (6)	0.3148 (3)	0.1080 (4)
C(28)	0.0978 (6)	0.3213 (3)	0.2161 (4)
C(101)	0.0161 (6)	0.0236 (3)	0.1748 (4)
C(102)	0.1564 (6)	0.0581 (3)	0.1823 (4)
C(103)	0.2483 (7)	0.0355 (3)	0.2677 (4)
C(104)	0.1694 (7)	−0.0122 (3)	0.3133 (5)
C(105)	0.0282 (7)	−0.0203 (3)	0.2570 (4)
C(201)	0.0167 (5)	0.1636 (3)	0.3334 (4)
C(202)	0.0971 (6)	0.1346 (3)	0.4193 (4)
C(203)	0.0028 (7)	0.0877 (3)	0.4553 (4)
C(204)	−0.1344 (7)	0.0864 (3)	0.3917 (4)
C(205)	−0.1266 (6)	0.1329 (3)	0.3159 (4)
N(1)	−0.1570 (5)	0.0732 (2)	0.0388 (3)
N(2)	0.0114 (4)	0.2692 (2)	0.2565 (3)
O(1)	−0.2112 (4)	−0.0208 (2)	0.1036 (3)
O(2)	0.2183 (4)	0.2085 (2)	0.2523 (3)
O(13)	−0.4207 (4)	0.1581 (2)	0.0305 (3)
O(16)	−0.3259 (4)	0.2419 (2)	0.1894 (3)
O(23)	0.0781 (4)	0.2055 (2)	−0.0421 (2)
O(26)	0.0020 (4)	0.3310 (2)	0.0406 (3)
O(900)	0.4062 (7)	0.0412 (3)	0.5522 (4)
O(910)	0.4253 (6)	0.0324 (3)	0.7636 (4)
H(901)	0.3912 (86)	0.0369 (37)	0.6301 (65)
H(902)	0.4979 (100)	0.0364 (39)	0.5273 (67)
H(911)	0.3344 (86)	0.0393 (41)	0.7929 (63)

Table IV. Selected Bond Distances and Angles with Estimated Standard Deviations for Fe(CpCONHMe)$_2$ (4a)

Fe(1)–C(11)	2.025 (4)	Fe(1)–C(12)	2.028 (4)
Fe(1)–C(13)	2.056 (4)	Fe(1)–C(14)	2.057 (5)
Fe(1)–C(15)	2.055 (5)	Fe(1)–C(21)	2.032 (4)
Fe(1)–C(22)	2.049 (4)	Fe(1)–C(23)	2.061 (5)
Fe(1)–C(24)	2.047 (5)	Fe(1)–C(25)	2.038 (5)
C(1)–C(11)	1.485 (6)	C(1)–N(1)	1.327 (6)
C(1)–O(1)	1.201 (6)	C(2)–C(21)	1.462 (6)
C(2)–N(2)	1.347 (6)	C(2)–O(2)	1.198 (6)
C(3)–N(1)	1.444 (6)	C(4)–N(2)	1.444 (6)
C(11)–C(12)	1.417 (6)	C(11)–C(15)	1.422 (7)
C(12)–C(13)	1.420 (7)	C(13)–C(14)	1.416 (8)
C(14)–C(15)	1.422 (6)	C(21)–C(22)	1.431 (7)
C(21)–C(25)	1.426 (6)	C(22)–C(23)	1.424 (7)
C(23)–C(24)	1.408 (8)	C(24)–C(25)	1.419 (7)
O(1)–C(1)–C(11)	123.6 (5)	O(1)–C(1)–N(1)	123.9 (5)
C(11)–C(1)–N(1)	112.4 (4)	N(2)–C(2)–C(21)	112.3 (4)
O(2)–C(2)–C(21)	125.2 (5)	O(2)–C(2)–N(2)	122.5 (5)
C(12)–C(11)–C(1)	127.6 (5)	C(15)–C(11)–C(1)	123.8 (4)
C(15)–C(11)–C(12)	108.5 (4)	C(13)–C(12)–C(11)	107.9 (4)
C(14)–C(13)–C(12)	107.8 (4)	C(15)–C(14)–C(13)	108.6 (5)
C(14)–C(15)–C(11)	107.2 (4)	C(22)–C(21)–C(2)	123.3 (4)
C(25)–C(21)–C(2)	128.4 (5)	C(25)–C(21)–C(22)	108.3 (4)
C(23)–C(22)–C(21)	107.1 (4)	C(24)–C(23)–C(22)	108.5 (5)
C(25)–C(24)–C(23)	108.7 (4)	C(24)–C(25)–C(21)	107.4 (5)
C(3)–N(1)–C(1)	116.0 (4)	C(4)–N(2)–C(2)	116.3 (4)

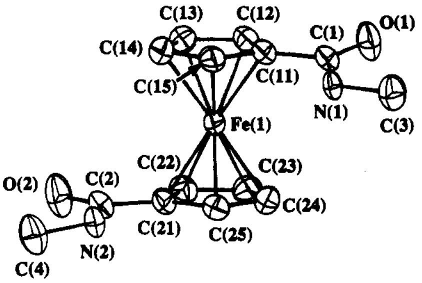

Figure 1. Molecular view of **4a** with thermal ellipsoids drawn at the 50% probability level. Hydrogen atoms have been omitted for clarity.

Table V. Selected Bond Distances and Angles with Estimated Standard Deviations for [Fc.2.2] (1)

Fe(1)–C(101)	2.033 (5)	Fe(1)–C(102)	2.039 (5)
Fe(1)–C(103)	2.052 (5)	Fe(1)–C(104)	2.052 (6)
Fe(1)–C(105)	2.039 (6)	Fe(1)–C(201)	2.049 (5)
Fe(1)–C(202)	2.029 (5)	Fe(1)–C(203)	2.038 (5)
Fe(1)–C(204)	2.042 (5)	Fe(1)–C(205)	2.044 (5)
C(1)–C(101)	1.496 (7)	C(1)–N(1)	1.344 (7)
C(1)–O(1)	1.244 (6)	C(2)–C(201)	1.506 (7)
C(2)–N(2)	1.353 (6)	C(2)–O(2)	1.223 (5)
C(11)–C(12)	1.506 (7)	C(11)–N(1)	1.469 (6)
C(12)–O(13)	1.416 (6)	C(14)–C(15)	1.487 (7)
C(14)–O(13)	1.412 (6)	C(15)–O(16)	1.424 (5)
C(17)–C(18)	1.509 (6)	C(17)–O(16)	1.404 (6)
C(18)–N(2)	1.482 (6)	C(21)–C(22)	1.525 (6)
C(21)–N(1)	1.465 (7)	C(22)–O(23)	1.422 (6)
C(24)–C(25)	1.499 (7)	C(24)–O(23)	1.422 (6)
C(25)–O(26)	1.433 (6)	C(27)–C(28)	1.500 (6)
C(27)–O(26)	1.436 (5)	C(28)–N(2)	1.475 (6)
C(101)–C(102)	1.437 (7)	C(101)–C(105)	1.432 (7)
C(102)–C(103)	1.417 (7)	C(103)–C(104)	1.399 (8)
C(104)–C(105)	1.405 (8)	C(201)–C(202)	1.427 (7)
C(201)–C(205)	1.425 (7)	C(202)–C(203)	1.411 (7)
C(203)–C(204)	1.412 (7)	C(204)–C(205)	1.417 (7)
O(900)–H(901)	1.06 (8)	O(900)–H(902)	0.91 (8)
O(910)–H(911)	0.94 (8)		
O(13)–O(16)	2.829 (5)	O(13)–O(23)	4.705 (5)
O(13)–O(26)	5.239 (5)	O(16)–O(23)	4.974 (5)
O(16)–O(26)	4.114 (5)	O(23)–O(26)	2.991 (5)
N(1)–C(1)–C(101)	122.5 (5)	O(1)–C(1)–C(101)	116.9 (5)
O(1)–C(1)–N(1)	120.6 (5)	N(2)–C(2)–C(201)	119.2 (5)
O(2)–C(2)–C(201)	119.7 (5)	O(2)–C(2)–N(2)	121.1 (5)
N(1)–C(11)–C(12)	112.9 (4)	O(13)–C(12)–C(11)	108.3 (5)
O(13)–C(14)–C(15)	107.7 (5)	O(16)–C(15)–C(14)	108.8 (5)
O(16)–C(17)–C(18)	109.9 (4)	N(2)–C(18)–C(17)	113.7 (4)
N(1)–C(21)–C(22)	112.4 (4)	O(23)–C(22)–C(21)	109.9 (4)
O(23)–C(24)–C(25)	110.4 (5)	O(26)–C(25)–C(24)	112.3 (4)
O(26)–C(27)–C(28)	110.4 (4)	N(2)–C(28)–C(27)	115.8 (4)
C(102)–C(101)–C(1)	133.9 (5)	C(105)–C(101)–C(1)	120.0 (5)
C(105)–C(101)–C(102)	106.1 (5)	C(103)–C(102)–C(101)	108.0 (5)
C(104)–C(103)–C(102)	108.7 (5)	C(105)–C(104)–C(103)	108.3 (6)
C(104)–C(105)–C(101)	108.9 (6)	C(202)–C(201)–C(2)	120.7 (4)
C(205)–C(201)–C(2)	131.8 (5)	C(205)–C(201)–C(202)	107.4 (5)
C(203)–C(202)–C(201)	108.1 (5)	C(204)–C(203)–C(202)	108.3 (5)
C(205)–C(204)–C(203)	108.3 (5)	C(204)–C(205)–C(201)	107.8 (5)
C(11)–N(1)–C(1)	116.9 (5)	C(21)–N(1)–C(1)	125.2 (4)
C(21)–N(1)–C(11)	116.9 (5)	C(18)–N(2)–C(2)	125.2 (4)
C(28)–N(2)–C(2)	116.2 (4)	C(28)–N(2)–C(18)	115.3 (4)
C(14)–O(13)–C(12)	114.9 (4)	C(17)–O(16)–C(15)	113.4 (4)
C(24)–O(23)–C(22)	112.7 (4)	C(27)–O(26)–C(25)	112.5 (4)
H(902)–O(900)–H(901)	122.7 (76)		

Table IV. The bond lengths and angles about the cyclopentadienyl rings vary little and are close to those reported for analogous ferrocenes.[27-32] The amide bond lengths are in good agreement with literature values.[33] The bisamide **4a** adopts an eclipsed 1,3′-conformation with the substituents located in a manner almost identical with

---

(27) (a) Dunitz, J. D.; Orgel, L. E.; Rich, A. *Acta Crystallogr.* **1956**, *9*, 373. (b) Dunitz, J.; Orgel, L. E. *Nature* **1953**, *171*, 121.

(28) Seibold, E. A.; Sutton, L. E. *J. Chem. Phys.* **1955**, *23*, 1967.

(29) Palenik, G. J. *Inorg. Chem.* **1970**, *9*, 2424.

(30) Palenik, G. J. *Inorg. Chem.* **1969**, *8*, 2744.

(31) Churchill, M. E.; Wormald, J. *Inorg. Chem.* **1969**, *3*, 716.

(32) Calverin, P. G.; Weigel, D. *Acta Crystallogr.* **1971**, *B27*, 1253.

(33) Sutton, L. E. *Table of Interatomic Distances and Configuration in Molecules and Ions*; Special Publication No. 18; The Chemical Society: London, 1965.

(34) Danks, I. P.; Hall, C. D.; Nyburg, S. C.; Parkins, A. W.; Sharpe, N. W. *Organometallics* **1990**, *9*, 1602.

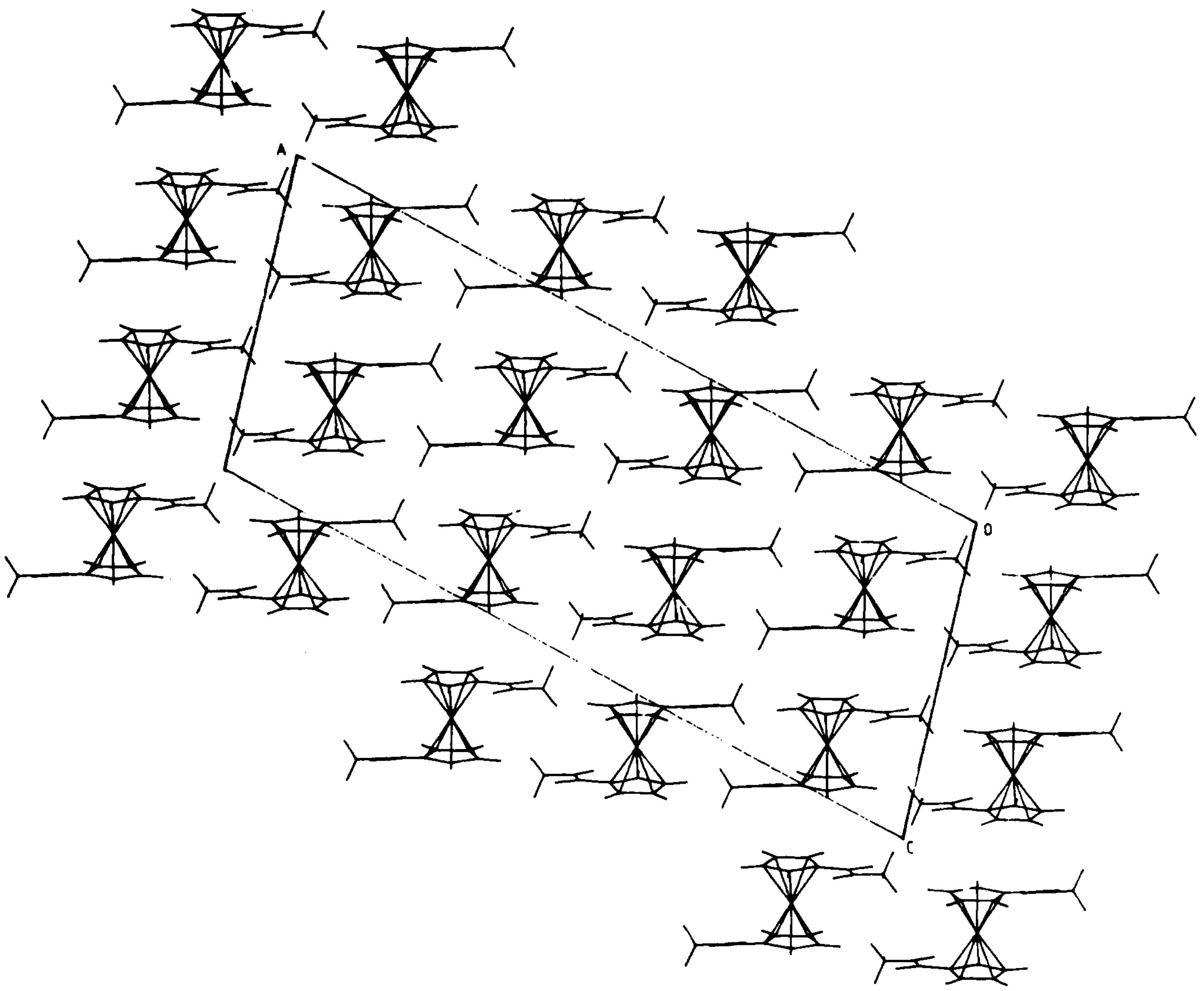

Figure 2. Packing diagram of **4a** as viewed down the b axis.

Table VI. Structural Angles (See Figure 3) in Disubstituted Ferrocenes

ferrocene derivative	α, deg	β,[a] deg Cp(1)	β,[a] deg Cp(2)	γ, deg	ref
1	1.1	15.7	50.2	79.1	this work
2	2.1	34.2	34.8	41.8	12a
	3.1	37.8	33.3	41.0	
3[b]	3.3			42.4	7a
4a	1.4	15.6	6.0	142.0	this work
5	1.0	11.5	8.9	139.3	29
6a	1.3	0.8	4.7	1.6	30
7	1.5	10.8	6.3	129.1	32
8	2.3			75.3	8a
9	1.8			71.4	8c
10a	2.4			7.8	8b
10b	3.4			6.7	8b
10c	0.3			3.1	8c

[a] Cp(1) = C(101) to C(105), and Cp(2) = C(201) to C(205) in **1**; Cp(1) = C(11) to C(15), and Cp(2) = C(21) to C(25) in **4a**. [b] As its NaSCN complex.

that previously reported[29] for 1,1′-diacetylferrocene (**5**). This minimizes steric repulsion between the substituents and allows very efficient packing in the unit cell, Figure 2.

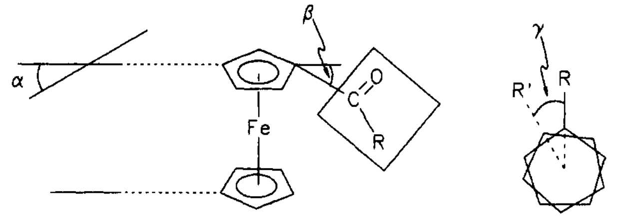

Figure 3. Schematic diagram depicting the angles α, β, γ as listed in Table V, α being a measure of the noncoplanarity of the two cyclopentadienyl rings, β the angle of the carbonyl group relative to the cyclopentadienyl ring, and γ the relative orientation of the two cyclopentadienyl rings in a ferrocene derivative.

The structural features of particular interest when comparing disubstituted ferrocenes, namely (i) α, the relative angle of tilt of the two cyclopentadienyl rings; (ii) β, the orientation of the carbonyl plane relative to the cyclopentadienyl ring; and (iii) γ, the relative disposition of the two cyclopentadienyl rings are shown schematically in Figure 3, and compared with the corresponding values found in other simple disubstituted ferrocenes in Table VI. For the related series of compounds **4a**, **5**, **6a**, and **7**, the carbonyl substituents are nearly coplanar with the

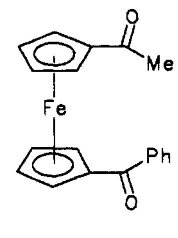

7

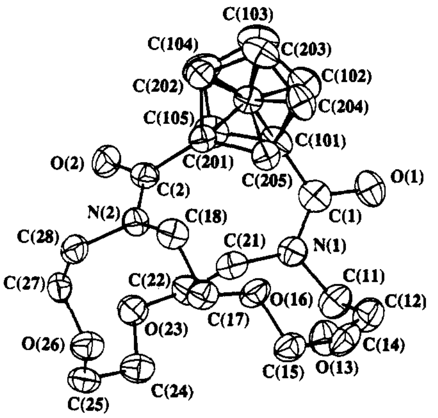

Figure 4. Molecular view of 1 with thermal ellipsoids drawn at the 50% probability level. The water molecules and hydrogen atoms have been omitted for clarity.

cyclopentadienyl rings, as indicated by the small values of β. In the absence of strong intermolecular forces (**6a** crystallizes as hydrogen-bonded dimeric units[30]) they all adopt 1,3′-conformations. The ideal value of γ for this situation is 144°. These values are presumably guided by crystal packing forces, although the near coplanarity of the cyclopentadienyl rings and carbonyl groups may be indicative of weak electronic interactions.

1,1′-[(1,4,10,13-Tetraoxa-7,16-diazacyclooctadecane-7,16-diyl)dicarbonyl]ferrocene Dihydrate [Fc.2.2], 1. Shortly after we had finished our work on this material, preliminary results of another X-ray structural study appeared,[13] but due to the higher precision of the present work, we feel justified in presenting our structural data here. The two determinations are similar, and only key results will be described. A view of the molecular structure is shown in Figure 4, and selected distances and angles are given in Table V.

The molecular dimensions of the ferrocene unit show no unusual behavior when compared with those of related ferrocenes,[27-32] and the two cyclopentadienyl rings are effectively coplanar (Table VI). This compound adopts a 1,2′-conformation with the cyclopentadienyl rings rotated from the eclipsed orientation by 7.1° (cf. 6.4° in ref 13). The adoption of a geometry similar to that found in the bisamide **4a** is prevented by the presence of a 1,1′-bridge. Similar 1,2′-conformations are found in the solid state for the ferrocenophanes **8** and **9**, whereas **10a–c** favor approximately 1,1′-eclipsed geometries (Table VI). The planes defined by the two amide units in 1 lie at considerably different angles (β) relative to the ferrocene ring, in marked contrast to the behavior of other, simpler, 1,1′-disubstituted derivatives. The carbonyl groups are also approximately trans relative to a vertical plane through the ferrocene ring. Consequently, only one of the amide carbonyl groups is oriented for efficient interaction with the cyclopentadienyl rings, and within the unit cell, there are two different carbonyl environments. Indeed it is likely that the very large value of β observed for ring 2 reflects distortion of the crown ether ring in order to minimize strain. Each of the amide units are approximately planar, thereby reducing the flexibility of the crown ether ring and making the nitrogen lone pairs unavailable for ion binding.

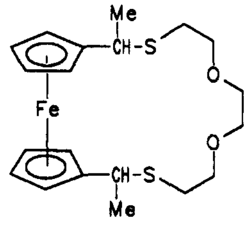

8

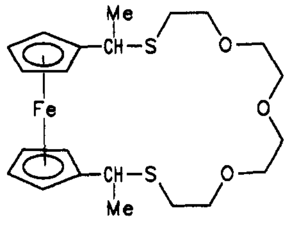

9

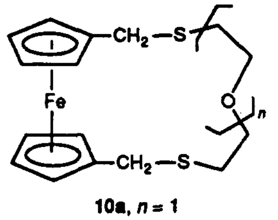

10a, $n = 1$
b, $n = 2$
c, $n = 3$

The nonequivalence of the two carbonyl environments in 1 is evident from the bond lengths about the two carbonyl carbon atoms determined in the present study (Table V). In Table VII, these results are compared with those reported for related structures. Our data indicate that the bonds of the amide units in 1 (and the related cryptands 2 and 11) have more single-bond character than was previously suggested,[13] both the C=O and C—N bonds being significantly longer than those in **4a**. This and the lengthening of the N-alkyl bonds may also reflect the considerable strain present in the ferrocene cryptand monomers. Interestingly, comparison with our data for the dimer 2[12] reveals that in the latter case all the bonds under consideration here are longer with the notable exception of N_1–C_{trans} (Table VII).

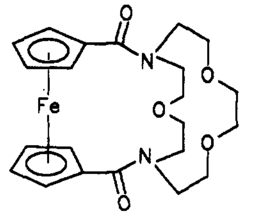

11

The primary purpose behind an X-ray structural study of 1 was to investigate the geometry of the ion-binding cavity. It is evident from Figure 4 that the chains containing the four ether oxygens adopt a rather twisted conformation in space and that there is a cleft between the chains which would allow *external* binding of an ion, i.e., remote from the ferrocene unit. The cavity defined by the ethereal oxygen atoms has internuclear (O–O) distances ranging from 2.83 to 5.24 Å. The very small internuclear distance between neighboring oxygens in each ether chain suggests that these chains are very compressed (i.e., O(13)–O(16) and O(23)–O(26) are both less than the sum of the van der Waals radii). If a similar conformation is present in solution, it would seem that only small metal ions should bind efficiently.

The crystals of 1 were found to contain two molecules of water per asymmetric unit. In an earlier report of the structure, the hydrogen atoms could not be located.[13] In this study, we have been able to identify and successfully refine the positions of three of the four hydrogen atoms and can give a more complete description of the hydrogen bonding. The two water molecules are linked via a hydrogen bond from O(910) to H(901) of 1.77 (8) Å. This dimeric unit is then linked to one of the carbonyl groups of the crown ether unit, O(1)–H(911) = 1.87 (8) Å. As seen in the packing diagram, Figure 5, the water molecules reside in tunnels that exist between the ferrocene cryptands. This hydrogen bonding appears to be important in stabilizing the packing of this structure as no anhydrous crystals could be produced.

Table VII. Comparison of Bond Lengths (Å) around Amide Units in Ferrocene Cryptands and Their Analogues

compd	4a	1	1	2	2	11
ref	*a*	*a*	13	12a	12b,c	34
$C_1{=}O_1$	1.201 (6)	1.244 (6)	1.225 (12)	1.28 (2)	1.24 (1)	1.215 (16)
	1.198 (6)	1.223 (5)	1.225 (12)	1.30 (2)	1.23 (1)	1.229 (18)
				1.27 (2)	1.23 (1)	
				1.33 (2)	1.26 (1)	
$C_1{-}N_1$	1.327 (6)	1.344 (7)	1.334 (13)	1.36 (2)	1.37 (1)	1.342 (17)
	1.347 (6)	1.353 (6)	1.339 (13)	1.37 (2)	1.38 (1)	1.356 (17)
				1.39 (2)	1.37 (1)	
				1.44 (2)	1.42 (2)	
$C_1{-}C_{11}$	1.485 (6)	1.496 (7)	1.472 (14)	1.53 (2)	1.54 (2)	1.469 (18)
	1.462 (6)	1.506 (7)	1.494 (14)	1.53 (2)	1.51 (2)	1.474 (19)
				1.51 (2)	1.52 (1)	
				1.49 (2)	1.50 (2)	
$N_1{-}C_{2cis}$	1.444 (6)	1.469 (6)	1.464 (12)	1.56 (2)	1.52 (1)	1.450 (19)[b]
	1.444 (6)	1.475 (6)	1.474 (11)	1.48 (2)	1.49 (1)	1.415 (22)[c]
				1.47 (2)	1.47 (1)	
				1.51 (2)	1.49 (1)	
$N_1{-}C_{2trans}$		1.465 (7)	1.494 (12)	1.32 (2)	1.41 (1)	1.430 (19)[c]
		1.482 (6)	1.485 (13)	1.30 (2)	1.41 (2)	1.468 (23)[b]
				1.41 (2)	1.41 (1)	
				1.26 (2)	1.39 (1)	

[a] This work. [b] $CH_2CH_2OCH_2CH_2$ chain. [c] $(CH_2CH_2O)_2CH_2CH_2$ chain.

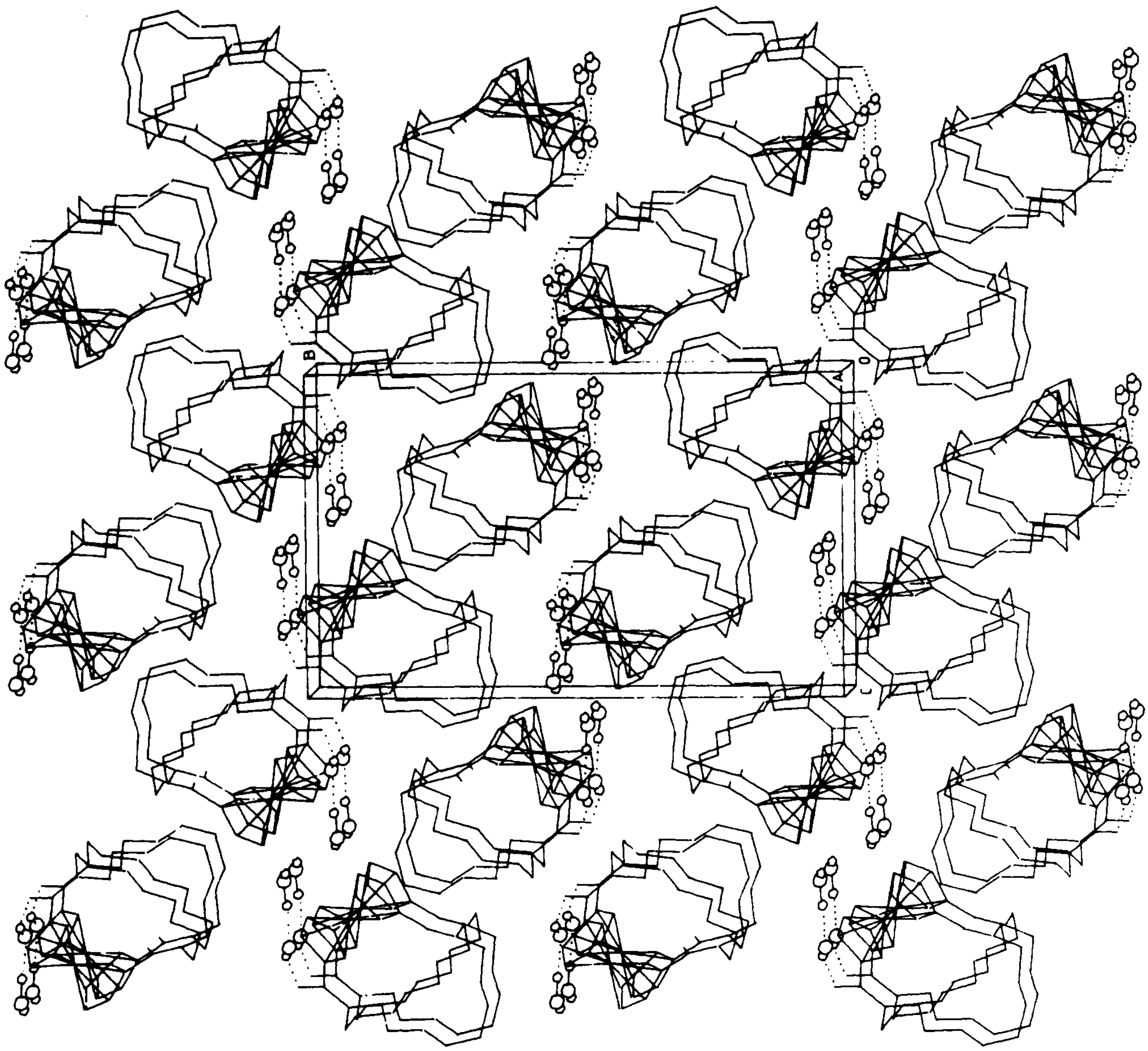

Figure 5. Packing diagram of 1 as viewed down the *a* axis. Hydrogen bonding is shown as dashed lines. The hydrogen atoms of the ferrocene moiety have been omitted for clarity.

Table VIII. ^{13}C CPMAS Solid-State NMR Spectra of a Series of 1,1′-Disubstituted Ferrocenes[a]

	δ (ferrocene carbons), ppm			
compd	C(1)/C(1′)	C(2)/C(2′)–C(5)/C(5′)	C=O	δ (side chain) others, ppm
4a	77.3	74.8, 71.2, 66.7	170.0	28.5 (NMe)
4b	80.7	71.5, 73.8, 76.2, 78.6	170.1	37.3 40.0 (NMe)
4c	78.6	72.5, 76.7	168.8	45.7 (NCH_2) 50.8 (NCH_2) 68.5 (OCH_2)
5	81.2	74.3 (v br)	204.5	29.2 (CH_3)
6a	75.2	74.5 (br)	176.5	
6b	75.2	72.5, 74.3	172.4	53.4 (OMe)
1[b]	84.9	72.0, 74.0, 76.4 77.9, 79.4	169.0 170.5	50.0 (NCH_2) 67.3 69.8 70.5 76.4 (OCH_2)

[a] Assignments based on solution data, aided by nonquaternary supression experiments. [b] *Recorded on the dihydrate.*

Solid-State NMR Studies. High-resolution solid-state ^{13}C NMR spectra often give rise to line multiplicities not observed in solution.[35,36] For example, while the spectra of crown ethers can be used for the determination of asymmetric units, interpretation of such spectra can be complicated by crystal packing phenomena or the existence of different crystalline forms in the solid state.[37] Very little work has of yet been reported on the solid-state NMR spectroscopy of ferrocenes and particularly the amides. Pines and co-workers[38] have studied chemical shielding parameters for a series of metallocenes, which included only reference to one substituted ferrocene, the decamethyl derivative.

We have applied cross-polarization/magic angle spinning (CPMAS) ^{13}C NMR techniques to a number of 1,1′-disubstituted ferrocenes, Table VIII, and have assigned the resonances by comparison with solution spectra. The spectrum of the bis(methylamide) **4a** shows one carbonyl and one methyl resonance together with four independent signals due to the cyclopentadienyl carbons, that due to the ipso carbon (C(1)/C(1′)) being assigned by nonquaternary suppression experiments. Solution chemical shifts are similar to those found in the solid-state spectrum with the exception of the methyl group, which is at significantly lower field in $CDCl_3$ solution (see Experimental Section). Comparison with the spectra of the bis(dimethylamide) **4b** is interesting, for in that case two methyl environments are evident in the CPMAS spectrum, whereas only one methyl resonance is observed in solution (22.5 MHz, $CDCl_3$—see Experimental Section) at a chemical shift (δ 38.3 ppm) intermediate between those found in the solid state. Finally, we have prepared 1,1-bis(*N*,*N*-morpholinocarbonyl)ferrocene (**4c**) as a better model for the ferrocene cryptands, e.g., **1**. Here doubling of the NCH_2 aliphatic resonances is clearly evident in the solid state (but again not in solution—see Experimental Section). Presumably the spectra of **4b** and **4c** reflect frozen rotation about the amide bonds; again only one carbonyl environment is observed in each case.

The solid-state NMR spectrum of 1,1′-diacetylferrocene (**5**) is similar to that found in solution though the resonances due to the ferrocenyl carbons merge into one broad adsorption. The spectrum of ferrocene-1,1′-dicarboxylic acid (**6a**) is rather different and shows one broad ferrocenyl and one relatively sharp carbonyl resonance, whereas that of the ester **6b** shows considerably more detail and compares well with that observed in solution. This perhaps reflects the high symmetry of the H-bonded dimer present in **6a**,[30] where an additional mirror plane bisects the cyclopentadienyl ring and reduces the number of expected ring resonances to three.

The solution ^{13}C NMR spectrum of **1** has been assigned by Hall and co-workers[39] and there is considerable correspondence between that and our CPMAS data. However, one notable feature of the solid-state spectrum is the clear presence of *two* carbonyl resonances of equal intensity, consistent with the two different carbonyl environments indicated by the crystallographic data. It is notable that in each of the other spectra of ferrocene carbonyl derivatives reported here, only one carbonyl absorption is observed, consistent with the structural data as discussed earlier. It should also be noted that **1** shows two amide carbonyl stretch bands in the solid state [ν_{max} (Nujol) 1610, 1619 cm^{-1}].

Ion-Extraction Experiments. In their original work on the [Fc.2.2] cryptand monomer (**1**), Bell and Hall[5] reported an ion-binding selectivity preference, as suggested by picrate salt extraction experiments, $Ca^{2+} \gg Li^+ > Na^+ \cong Mg^{2+} \gg K^+ \cong 0$. The alkali-metal selectivity sequence suggests a very small binding cavity, but the large preference for Ca^{2+} (and to a lesser extent the similarity in the behavior of the Mg^{2+} and Na^+ salts) would appear to be anomalous. The X-ray structural data above reveal a very small cavity available for ion encapsulation within this cryptand, the amide nitrogen atoms being apparently unavailable for binding, and the four ether-bridge oxygens forming a cavity having a diameter of ca. 2.1 Å (calculated from distances between atom centers less the van der Waals' radii of the oxygen atoms). This is significantly smaller, for example, than that seen in 18-crown-6 (ca. 2.8 Å[40]). Another explanation for the picrate extraction sequence might, for example, be that H_3O^+ is being complexed as its picrate salt in preference to the alkaline-earth cation. Alternatively, larger ions may be accommodated externally by the cleft.

Beer et al.[41] have recently investigated complex formation between alkali-metal cations and ferrocene bisamides including **4a–c**. Their results suggest that while **4b** forms 2:1 (amide:M^+) complexes with Li^+ by coordination with the carbonyl group, there is no evidence for binding of Na^+ and K^+ by such amides. They also failed to detect any binding of Li^+ by the [2.2]ferrocene monomer **1** in acetonitrile.

We have examined extraction by **1** of hydroxypyridone trimethine oxonol salts **13**[12c,20] from aqueous solution into dichloromethane. Such dye salts benefit from having higher extinction coefficients, and reduced hazard when

---

(35) (a) Yannoni, C. S. *Acc. Chem. Res.* **1982**, *15*, 201. (b) Wasylishan, R. E.; Fyfe, C. A. *Annu. Rev. NMR Spectrosc.* **1982**, *12*, 1. (c) Balimann, G. E.; Groombridge, C. J.; Harris, R. K.; Packer, K. J.; Say, B. J.; Tanner, S. F. *Philos. Trans. R. Soc. London, Ser. A* **1981**, *299*, 643.

(36) Belton, P. S.; Tanner, S. F.; Wright, K. H.; Owen, J. D.; Payne, M. P.; Truter, M. R.; Wingfield, J. N. *Inorg. Chim. Acta* **1983**, *77*, L201.

(37) (a) Buchanan, G. W.; Kirby, R. A.; Charland, J. P. *J. Am. Chem. Soc.* **1988**, *110*, 2477. (b) Buchanan, G. W.; Kirby, R. A.; Bourque, K. K.; Morat, C. *Can. J. Chem.* **1988**, *66*, 2204.

(38) (a) Wemmer, D. E.; Pines, A. *J. Am. Chem. Soc.* **1981**, *103*, 34. (b) Wemmer, D. E.; Ruben, D. J.; Pines, A. *J. Am. Chem. Soc.* **1981**, *103*, 28.

(39) Hammond, P. J.; Beer, P. D.; Hall, C. D. *J. Chem. Soc., Perkin Trans. 1* **1984**, 707.

(40) (a) Dunitz, J. D.; Dobler, M.; Seiler, P.; Phizackerley, R. P. *Acta Crystallogr.* **1974**, *B30*, 2733. (b) Pedersen, C. J. *Fed. Proc., Fed. Am. Soc. Exp. Biol.* **1968**, *27*, 1305. (c) Frensdorff, H. K. *J. Am. Chem. Soc.* **1971**, *93*, 600. (d) Takeda, Y.; Goto, H. *Bull. Chem. Soc. Jpn.* **1979**, *52*, 1920.

(41) Beer, P. D.; Sikanyika, H.; Blackburn, C.; McAleer, J. F. *J. Organomet. Chem.* **1988**, *350*, C15.

(42) (a) Hall, C. D.; Sharpe, N. W.; Danks, I. P.; Sang, Y. P. *J. Chem. Soc., Chem. Commun.* **1989**, 419. (b) Hall, C. D.; Danks, I. P.; Sharpe, N. W. *J. Organomet. Chem.*, in press. (c) Hall, C. D.; Danks, I. P.; Lubienski, M. C.; Sharpe, N. W. *J. Organomet. Chem.* **1990**, *384*, 139.

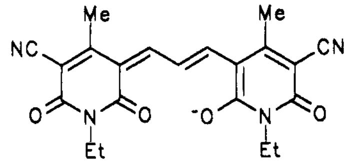

13 $^{1}/_{n}$ M^{n+}

compared with picrates, but are more difficult to synthesize and purify (they were recrystallized to constant extinction coefficient prior to use in these experiments). A series of control experiments using dibenzo-18-crown-6 showed that no dye is extracted into dichloromethane unless the crown ether is present and that the "normal" extraction preferences[40] are observed. For the ferrocene cryptand monomer 1, cations are extracted: $Li^+ > Mg^{2+} \sim Na^+ > Ca^{2+} > K^+ \sim NH_4^+$. Such behavior is more in line with that expected on the basis of the X-ray structural data for 1 than that originally observed[5] and suggests that in 1 the diaza-18-crown-6 moiety is rather compressed, leading to a small and relatively rigid cation receptor site that has low binding efficiency. Indeed the behavior of this macrocycle is typical of that expected of, for example, 12- or 14-crown-4.[37] In view of these observations, we have investigated further Li^+ ion binding by the [2.2]ferrocene monomer 1.

Preparation of and Spectroscopic Studies on Cryptates Derived from 1. We have prepared and characterized a number of lithium cryptate salts **12** of the [2.2]ferrocene monomer 1. The perchlorate **12a**, the iodide **12b**, and the trifluoromethanesulfonate **12c** each gave good combustion analysis data, suggesting 1:1 stoichiometry, but none of these materials crystallized well enough to produce single crystals suitable for X-ray structural study. Attempts to isolate complexes of 1 with calcium trifluoromethanesulfonate and $Li^+TCNQ^{\bullet -}$ (tetracyano-*p*-quinodimethane)[43] gave only poor yields of solid for which no satisfactory analytical data have been obtained.

Fast atom bombardment (FAB) mass spectroscopic studies[44] of the perchlorate **12a** are interesting for they show strong peaks at *m/e* 500 and 507, consistent with the presence of the ligand 1 and its Li^+–cryptate complex. In addition, there is a strong peak at *m/e* 1008, suggesting the presence of a lithium ion complexed with two molecules of the cryptand 1 (together with a hydrogen atom from the matrix).

We have used a number of spectroscopic techniques to investigate the nature of the cryptates **12**.

NMR Spectroscopic Studies. Live and Chan[45] have used both ^1H and ^{13}C NMR spectroscopy to elucidate the structures of a number of crown ether complexes, but Akabori et al.[46] found only very small spectral shifts ($\Delta\delta < 0.05$ ppm) when polyoxa-(*n*)-ferrocenophanes were complexed with a series of alkali-metal thiocyanates, which were attributed to electronic and conformational effects. Both sets of workers also noted the sensitivity of such spectral changes to solvent effects. The formation of 2:1 (host:guest) complexes of 1 with a number of divalent and trivalent metal ions has recently been reported by Hall.[42b] This is accompanied by, for example, significant changes in the ^{13}C NMR spectra that are particularly associated with carbonyl, ferrocene-C_1, and NCH_2 carbons (see Table IX). These results suggest that, in such cases, ion binding is external to the cryptand cavity and involves the carbonyl groups.

Table IX. Chemical Shift Changes Observed in the ^{13}C NMR Spectra of 1 (at Ambient Temperature) upon Complexation with $LiClO_4$ (Using the Assignments of Hall et al.[5,12])

	$\delta(^{13}C)$, ±0.03 ppm				
complex (solvent)	C=O	ipso-C	FeC	OCH_2	NCH_2
(a) Li^+ Ion Complexation by 1 (This Work)					
1 (CD_3OD)	170.86	78.44	70.37 71.20 71.64 72.62	68.66 69.16 69.60 71.49	48.53 50.89
12a (CD_3OD)	171.0	78.50	70.36 71.23 71.63 72.03	68.68 69.21 69.73 71.37	48.53 50.96
1 ($CDCl_3$)	170.69	78.73	71.10 71.41 72.79 73.24	69.37 70.02 70.47 72.78	50.06 51.42
12a ($CDCl_3$)	170.88	79.05	71.19 71.32 72.69 73.16	69.65 69.85 70.29 72.40	49.89 51.43
(b) Comparative Data for Mg^{2+} Complexation (See Ref 42c)					
1 (in $CD_3CN/CDCl_3$)	170.7	79.9			49.8 48.9
1 + Mg^{2+} (1:1) (in $CD_3CN/CDCl_3$)	175.0	81.4	70.9 72.2 72.9 75.7	77.1 70.5 70.9 71.9	50.1 51.9
1 + Mg^{2+} (2:1) (in $CD_3CN/CDCl_3$)	171.5	80.4	70.9 72.1 73.1 73.3	69.7 70.3 70.6 71.5	48.8 51.1

Differences observed upon complexation in the solution ^1H and ^{13}C NMR spectra of the monomer 1 and its $LiClO_4$ complex **12a** are reported in Table IX. Only small solvent-dependent chemical shift changes are evident (larger in $CHCl_3$ than in CD_3OD solvent), which appear mainly to be associated with the middle sections of the ethyleneoxy bridges (based on the assignments of Hall et al.[9,47]). Slight spectral reorganization is evident in the ^1H NMR spectrum of the complex **12a**. In the ^{13}C NMR spectrum in CD_3OD, the greatest effects are associated with C(3), C(4), and the carbonyl group, whereas in $CDCl_3$ the changes observed are for C(3)/C(4) and to a lesser extent C(2)/C(5), C(1), and the C=O group. In the latter case, however, such effects are significantly smaller than those reported by Hall.[42c] No major changes were observed in the spectra of the complex **12a** over the temperature range −50 to +50 °C.

Infrared Spectra.[48] Another notable feature of the infrared spectra of the M^{2+} complexes of 1 is the dramatic shift in ν_{max} (C=O), from 1615 to 1560 (1:1 complex) or 1600 cm^{-1} (2:1 complex).[42c] No comparable shift is observed in the spectrum of **12a**, which has ν_{max} 1610 cm^{-1}.

^7Li NMR Studies. Shamsipur and Popov[49] have observed an inverse relationship between the stability of

---

[43] Melby, L. R.; Harder, R. J.; Hertler, W. R.; Mahler, W.; Benson, R. E.; Mochel, W. E. *J. Am. Chem. Soc.* **1962**, *84*, 374.

[44] Fast atom bombardment (FAB) mass spectrometry has been used by Johnstone and Rose[44a] and Beer[44b] to investigate metal ion complexing by crown ethers and cryptands: (a) Johnstone, R. A. W.; Rose, M. E. *J. Chem. Soc., Chem. Commun.* **1983**, 1268. (b) Beer, P. D. *J. Chem. Soc., Chem. Commun.* **1985**, 1115.

[45] Live, D.; Chan, S. I. *J. Am. Chem. Soc.* **1976**, *98*, 3769.

[46] Akabori, S.; Shibahara, S.; Habata, Y.; Sato, M. *Bull. Chem. Soc. Jpn.* **1984**, *57*, 63. Akabori, S.; Habata, Y.; Sato, M. *Bull. Chem. Soc. Jpn.* **1984**, *57*, 68. Akabori, S.; Habata, Y.; Sakamoto, Y.; Sato, M.; Ebine, S. *Bull. Chem. Soc. Jpn.* **1983**, *56*, 537.

[47] Beer, P. D.; Elliot, J. E.; Hammond, P. J.; Dudman, C.; Hall, C. D. *J. Organomet. Chem.* **1984**, *263*, C37.

[48] Significant changes are observed in the infrared spectrum of 18-crown-6 when complexed with KSCN; see: Pederson, C. J. *J. Am. Chem. Soc.* **1967**, *89*, 2495, 7017.

[49] Shamsipur, M.; Popov, A. I. *Inorg. Chim. Acta* **1980**, *43*, 243.

Table X. ^{7}Li Chemical Shift Changes upon Addition of 1 mol Equiv of Ligand to 0.025 M Lithium Salt

solvent		$\Delta\delta(^7\text{Li})$, ppm			
ligand	salt	12-crown-4	15-crown-5	18-crown-6	1
MeOH	$LiClO_4$	0.11	0.11	0.17	0.11
	LiTCNQ	0.03	0.48	0.11	0.03
THF	$LiClO_4$	0.37	0.81	0.45	0.36
	LiTCNQ	0.11	0.70	0.33	0.13
	LiI	0.24	1.05	0.28	0.24
pyridine	LiI	0.15	0.91	0.21	0.15

lithium complexes of 18-crown-6 and diaza-18-crown-6 and the donicity of the solvent.[50] Following the same procedure, we have compared the complexing of $LiClO_4$, LiTCNQ, and LiI with the [2.2]ferrocene cryptand monomer 1, 12-crown-4, 15-crown-5, and 18-crown-6, in rigorously predried methanol, THF, and pyridine, by ^{7}Li NMR spectroscopy (Table X). These experiments suggest that the [2.2]ferrocene cryptand monomer shows a similar binding capacity to 12-crown-4. Only one ^{7}Li signal is observed, the chemical shift of which is dependent on the relative concentrations of ligand and lithium salt, indicating fast exchange between the different lithium environments on the NMR time scale (and relatively poor complexing by 1).[49] Ceraso and Dye[51] have demonstrated that addition of ethylenediamine slows the rate of Na^+ ion exchange between solution and [2.2.2]cryptand as observed by ^{23}Na NMR. No such effects are observed when this experiment is repeated using the [2.2]ferrocene cryptand monomer 1.

Our NMR experiments would seem to support the conclusions already drawn, i.e., that, despite its apparently greater size, the cavity in the [2.2]ferrocene cryptand monomer 1 behaves toward Li^+ in a manner similar to that of 12-crown-4. However, it should be noted that Shamsipur and Popov[49] found similar behavior for diaza-18-crown-6 when compared with 18-crown-6 itself, the former also showing an ion preference of $Li^+ > Na^+ > K^+$.

The small changes observed when the spectra of 1 and **12a** in CD_3OD are compared probably reflect dissociation of the complex **12a**, the alcohol solvent competing more efficiently for the cation than does $CDCl_3$.

Mössbauer Spectroscopic Studies. Akabori and coworkers[46] have used Mössbauer spectroscopy to investigate possible interaction of an encapsulated cation with a ferrocene macrocycle. They observed an increased quadrupole splitting when a metal ion is complexed with the crown ether **3** which they have tentatively ascribed to direct interaction between the metal cation (Li^+ or Na^+) and the iron atom. We have compared the Mössbauer spectra of solid samples of the [2.2]ferrocene monomer 1 and its lithium perchlorate salt **12a** but could detect *no* spectral change in this case, suggesting no direct interaction between Li^+ and the iron atom.

Conclusions

From the results presented here, we conclude that the ferrocene cryptand monomer 1 has a relatively small ion-binding cavity that can complex Li^+ ions through the ethyleneoxy bridges. There is no evidence for involvement of the ferrocene moiety or the carbonyl groups in such binding. This behavior contrasts markedly with that reported elsewhere[42] for association of 1 with larger and more highly charged metal ions where interaction with the carbonyl oxygens is clearly important. In this latter case, metal ion binding may well be external to the cryptand cavity involving, for example, a cleftlike conformation similar to that found for 1 in the solid state; such a structure would also facilitate the formation of 2:1 (host:guest) complexes. Work is underway to prepare crystals of a lithium cyprate of 1 suitable for X-ray structural study and to investigate in detail the energetics of lithium ion binding by 1.

Acknowledgment. We thank Dr. C. D. Hall for helpful advice and comments and for allowing us access to some of his results prior to publication. Thanks are also due to the SERC for a studentship to S.C.W.; Dr. C. Groombridge and Mr. D. Butler of the ULIRS CP/MAS NMR Service at Royal Holloway and Bedford New College for their help in obtaining solid-state NMR spectra; to Mr. W. Marshall of the ULIRS Mössbauer Service at Birbeck College, University of London; to Dr. G. E. Hawkes and Mr. P. Haycock of the ULIRS High Field Solution NMR Service at Queen Mary College, University of London; and Mr. M. Draper and Dr. D. Parkinson (RHBNC) for low-field NMR spectra.

Registry No. 1, 71818-07-0; $1\cdot2H_2O$, 119201-17-1; **4a**, 52293-41-1; **4b**, 107139-35-5; **4c**, 77788-06-8; **5**, 1273-94-5; **6a**, 1293-87-4; **6b**, 1273-95-6; **12** (X^- = TCNQ), 131657-07-3; **12a**, 131656-97-8; **12b**, 131656-98-9; **12c**, 131656-99-0; **13** (M = Li), 131657-03-9; **13** (M = Mg), 131657-04-0; **13** (M = Na), 131657-00-6; **13** (M = Ca), 110930-95-5; **13** (M = K), 131657-01-7; **13** (M = NH_4), 131657-02-8; 12-crown-4, 294-93-9; 15-crown-5, 33100-27-5; 18-crown-6, 17455-13-9; LiTCNQ, 1283-90-5; ^{7}Li, 13982-05-3; [Li·18-crown-6]ClO_4, 74065-10-4; [Li·15-crown-5]ClO_4, 74060-73-4; [Li·12-crown-4]ClO_4, 74048-82-1; [Li·12-crown-4]TCNQ, 74230-38-9; [Li·15-crown-5]TCNQ, 131657-05-1; [Li·18-crown-6]TCNQ, 131657-06-2; [Li·12-crown-4]I, 131657-08-4; [Li·15-crown-5]I, 131657-09-5; [Li·18-crown-6]I, 100676-80-0; 1,1′-bis(chlorocarbonyl)ferrocene, 12288-74-3.

Supplementary Material Available: Tables of positional parameters, bond lengths, bond angles, anisotropic thermal parameters, and least-squares planes for 1,1′-bis(*N*-methylcarbamyl)ferrocene (**4a**) and 1,1′-[(1,4,10,13-tetraoxa-7,16-diazacyclooctadecane-7,16-diyl)dicarbonyl]ferrocene dihydrate (**1**) (12 pages); tables listing observed and calculated structure factors (15 pages). Ordering information is given on any current masthead page.

---

(50) Gutmann, V. *Co-ordination Chemistry in Non-aqueous Solvents*; Springer-Verlag: Vienna, 1968.

(51) Ceraso, J. M.; Dye, J. L. *J. Am. Chem. Soc.* **1977**, *95*, 4432.